CEAS-GNC-2024-021

EuroGNC Navigation Guidance Control CEAS Bristol, UK June 11th-13th 2024
University of BRISTOL ROYAL AERONAUTICAL SOCIETY AIAA

Power Optimisation of Variable-Pitch Propeller for an IC Engine with Variable-RPM

Rohith S K PhD Scholar, Department of Aerospace Engineering, Indian Institute of Technology Madras, Chennai 600 036, India. rohithiitm.84@gmail.com

Bharath Govindarajan Assistant Professor, Department of Aerospace Engineering, Indian Institute of Technology Madras, Chennai 600 036, India. bharath@iitm.ac.in

Ramakrishna P A Professor, Department of Aerospace Engineering, Indian Institute of Technology Madras, Chennai 600 036, India. parama@iitm.ac.in

ABSTRACT

The present work studies the effect of a simultaneous variable pitch and variable RPM propeller on the thrust generated and aerodynamic power consumed. The study is motivated by the need for aerodynamic efficiency of vertical takeoff and landing systems, which are required to operate in hover (high thrust, no freestream) and cruise (low thrust, high flight speed) conditions. As all flight conditions considered are axial, a blade element momentum theory (BEMT) analysis was developed and employed to understand the aerodynamic behaviour in both these conditions. The BEMT methodology was validated against multiple propellers and was deemed to be appropriate for this work. For a given thrust condition, there are multiple combinations of RPM and blade pitch, and consequently, a gradient-based non-linear optimization technique was employed to identify the combination of RPM and pitch that results in the lowest power requirement. The current BEMT formulation uses linear aerodynamics, and therefore, to ensure the results obtained are practical, inequality constraints were imposed to limit the lift coefficient seen by the blade sections. It was observed that the optimization strategy was able to successfully predict the inputs (RPM and pitch) for all conditions considered. Studies were performed on the effect of varying RPM and flight speed on thrust and power. It was noted that a change in pitch is aerodynamically more efficient than a change in RPM as the latter results in a significant change in the local dynamic pressure, which increases the drag and the power required.

Keywords: UAV, IC engine, VPP, Optimisation

Nomenclature

θ_0	=	blade pitch, deg
N	=	Speed, RPM
Vc	=	climb velocity/forward speed, m/s
VPP	=	variable pitch propeller
$BEMT$	=	blade element momentum theory

1 Introduction and Motivation

The role of unmanned aerial vehicles (UAVs) has rapidly expanded into the civilian and military space, owing to technological developments in the powertrain and miniaturization of components in the last two decades. Armed forces and paramilitary groups use these vehicles in combat roles such as weapon delivery, communication relay, and swarming. They are also used in the civilian, agricultural, and medical sectors. One of the key goals of these designs is always the need for a higher range and endurance to service the various mission profiles. While there has been significant improvement in battery chemistry towards UAVs, the energy density at the pack level is approximately 200 W-hr/kg. Consequently, employing an all-electric powertrain will limit the range and endurance of UAV concepts owing to the increase in battery weight.

A potential way to increase operational time is through the use of internal combustion (IC) engines, which has a higher energy density of hydrocarbon-based fuels, compared to the battery [1]. IC engines as a powerplant has been used extensively for manned aircraft. Recent developments have also seen the use of these engines on fixed-wing and rotary-wing UAVs, as shown in Fig. 1.

Fig. 1 Various UAV concepts that utilize IC engines.

Additionally, there has been a demand for aerodynamically hybrid aircraft, i.e., those that are capable of both efficient Vertical Take-off & Landing (VTOL) and efficient cruise. Tilt-wing, tail-sitters and tilt rotors are a few vehicle configurations that operate in this fashion [2, 3]. On one hand, these flight modes require them to operate at low-speed and high-thrust settings during the hover/axial climb, and on the other hand, in cruise, the thrust required is low (only to counteract vehicle drag), but the cruise velocity is high. Traditional systems, such as helicopters, use variable pitch propellers (VPP), but they operate at a fixed RPM. The latter is a consequence of:: 1. the efficiency of the gas turbine engine at a fixed RPM, and 2. the aeroelastic effects of the flexible blades at other RPMs. Smaller scale rotors that use fixed pitch propellers (mechanically simpler) BLDC motors are free from the aforementioned constraints and hence utilize variable RPM systems. However, the fixed pitch ensures that these rotors/propellers are efficient only at a particular operating condition. Generally, low-pitch propellers are used for low-speed VTOL aircraft and high-pitch propellers for high-speed fixed-wing aircraft [4].

Figure 2 shows a blade section of a propeller, where the angle of attack is dependent on the blade pitch (θ) and inflow angle (ϕ). The former is set based on geometry and control input, and the latter is a function of the forward speed of the propeller, the rotational speed of the propeller, and the aerodynamics. An increase in forward speed decreases the angle of attack, and an increase in rotational speed increases the angle of attack. For the same blade pitch angle, an increase in forward flight speed increases the inflow angle which reduces the angle of attack. The blade section may also see negative angles of attack. If however, the blade pitch is trimmed for forward flight, a reduction in flight speed to hover, will see the angle of attack increase to the point of stall. Consequently, a propeller that can vary the blade pitch based on the flight condition is essential to ensure efficient operation across both flight modes [5].

Several authors have worked on variable-pitch propellers (VPP) powered by electric motors in the past [6, 7]. Podsedkowski et al. [8] have reported a 31% increase in thrust with a 12.5° increase in pitch

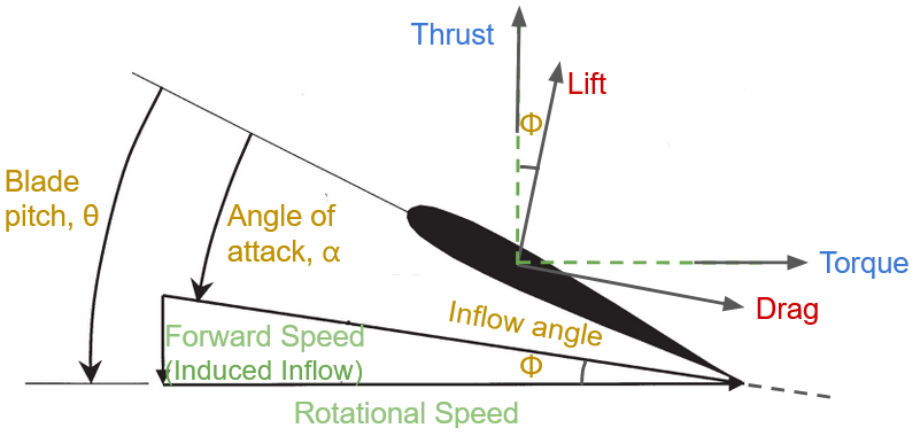

Fig. 2 Blade section of a propeller highlighting the aerodynamic environment.

under hover conditions compared to the thrust generated at default blade pitch settings of the propeller, and Jianhua Xu et al. [9] also reported an increase in the thrust up to 80% by using VPPs at 10 km altitude and 10 m/s wind compared to the thrust generated from a fixed-pitch propeller. A study by Tao Pang et al. [10] reported an increase in the thrust by 63% when the pitch was increased by 5 degrees when the IC engine was used under hover conditions compared to the thrust generated at 10 deg blade pitch. Many works [6, 11] have studied the power optimisation using VPP for the electric motor, but none optimised power required for IC engines, particularly with variable-pitch and variable RPM. Vishnu S Chipade et al. [12] worked on a VPP-based quadrotor system powered by a single gasoline engine in the centre through gear systems. Experimental testing of VPP with motor showed that the thrust generated increased by 20% with blade pitch increase by 2 deg when compared with thrust generated at 14 deg blade pitch.

The focus of the present work is to create an analytical model for VPP using blade element momentum theory powered by an IC engine. The study will focus on variable RPM and variable pitch for a proprotor in representative hover and cruise conditions. It is expected that there are multiple combinations of RPM and pitch to produce the same value of thrust, however, these operating conditions may be different in the amount of power required, which translates to varying levels of fuel consumption. Hence, this study proposes to identify the pitch and RPM for the least fuel consumption based on the demanded thrust based on formal optimisation techniques. The upcoming sections will explain the steps for theoretical testing for this study.

2 Blade Element Momentum Theory

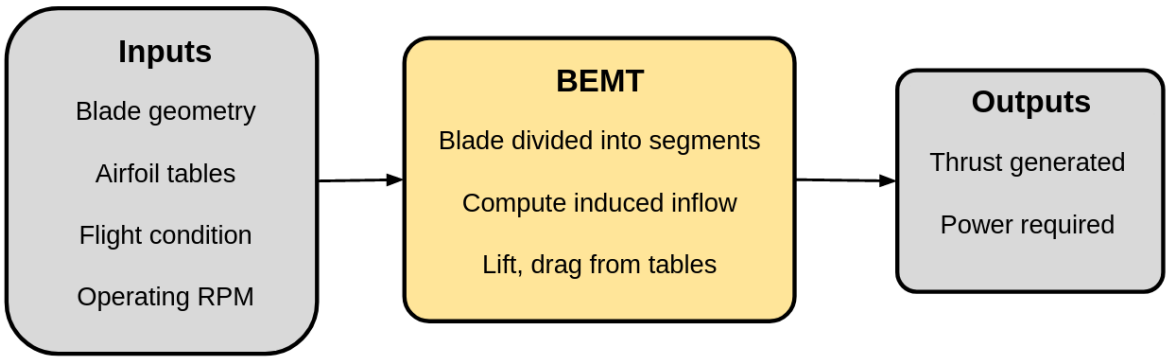

Fig. 3 Flowchart showing the basic elements of BEMT

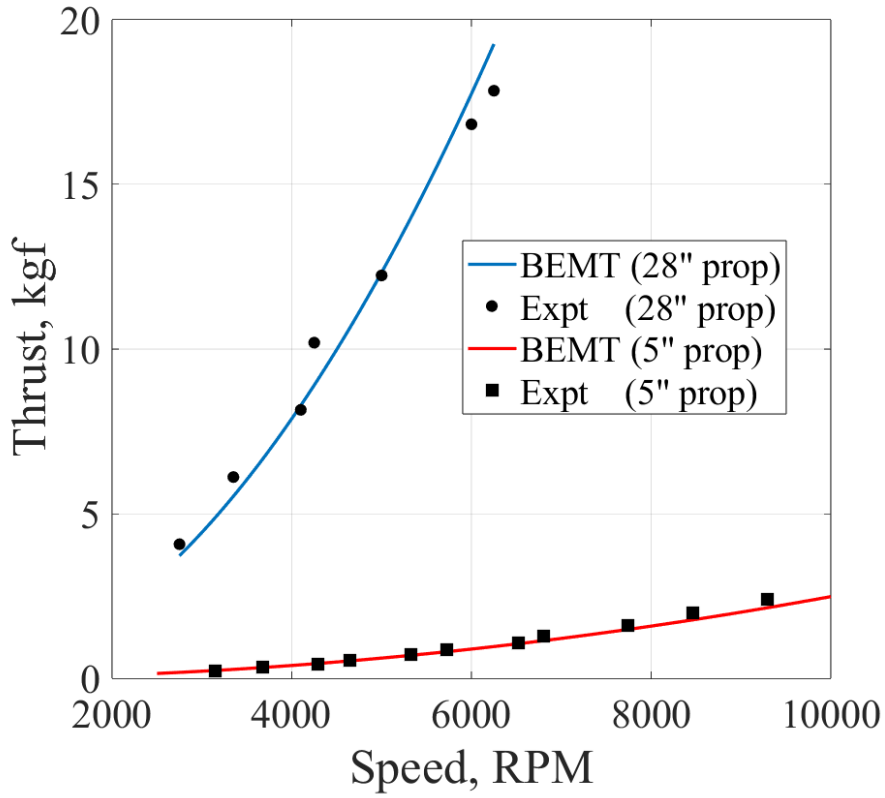

Fig. 4 Comparison of thrust vs RPM between experiments [14, 15] and BEMT

As the flight conditions considered are axial, Blade Element Momentum Theory (BEMT) [13] is used for estimating the thrust and the power for a given rotor geometry and flight condition. A large angle formulation is employed along with the assumption of 2D airfoils along each section. Along with the spanwise distribution of various airloads, integrated quantities such as thrust and power are also obtained, as shown in the schematic in Fig. 3. Blade geometries, fluid properties, operating RPM and airfoil properties are inputs for BEMT, while the integrated thrust generated and aerodynamic power (or torque) required are the outputs.

Towards validation efforts, a two-bladed wooden propeller was used, which is shown in Fig. 5(a) along with its chord and twist distributions. whose diameter is 28 inches. The chord and twist values were determined from the propeller and fit is shown. The chord and twist values at 75% span are 0.0452 m and 10.36 deg respectively. Figure 4 shows the comparison of the BEMT formulation against the 28-inch fixed-pitch variable-RPM IC-engine driven propeller and a 5-inch motor-driven propeller, where the solid lines represent BEMT predictions, and the circles denote experimental data of 28-inch propeller [14] and squares denote data of a 5-inch propeller. Good agreement was obtained between the two methods, lending confidence to the BEMT formulation. Further analysis for the preliminary study has been carried out using these blade properties.

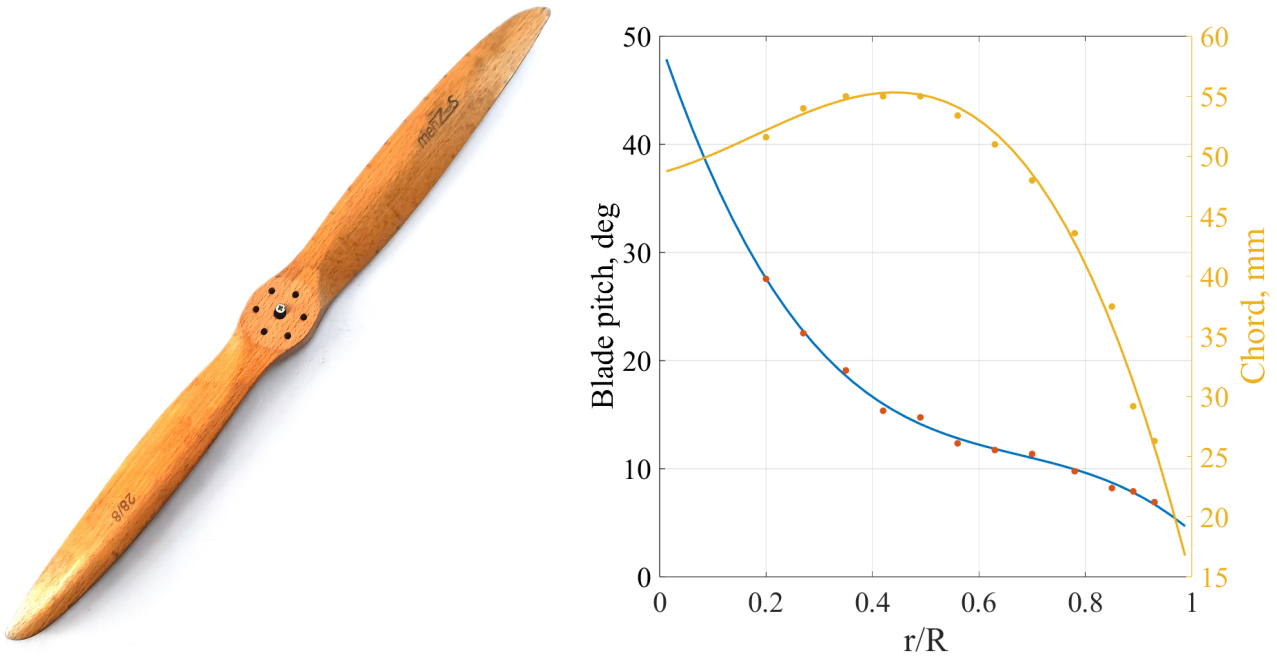

(a) Propeller (b) Geometry

Fig. 5 Image of the two-bladed propeller used along with the chord and twist distributions.

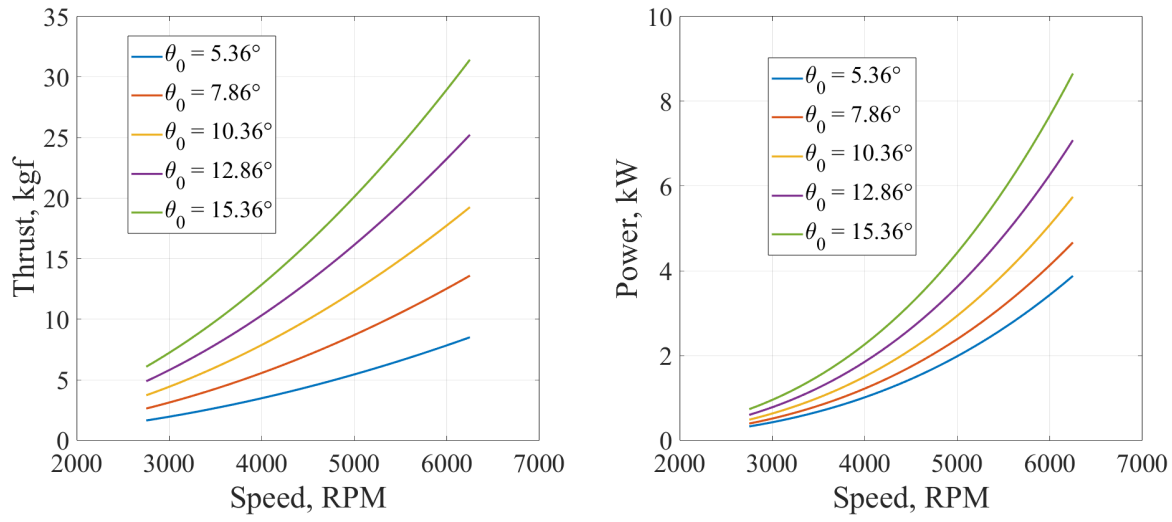

(a) Thrust (b) Power

Fig. 6 Variation of thrust generated and aerodynamic power at various RPM at different pitch angles (referenced to 75% span)

3 Results and Discussion

3.1 Effect of blade pitch and propeller RPM

Figures 6(a) and 6(b) show the static thrust generated and aerodynamic power required against various RPM and blade pitches (referenced to 75% span), respectively. BEMT analysis was carried out to predict thrust and power for different pitch values such as 2.5° and 5° increase and decrease from 10.4°. An increase in θ_0 results in an effective increase in the angle of attack (α), as shown in Fig. 2, increasing the lift and drag, which in turn increases the thrust and torque. This increase in torque increases the engine power required to drive the propeller. For instance, at a constant engine RPM of 4,500, an increase in θ_0 from 5.36° to 15.36° increases thrust generated from 4.5 kgf to 16.6 kg and power required increases from 1.5 kW and 3.3 kW. Similarly, when blade pitch is maintained constant say 10.4°, increasing engine/propeller RPM from 4,000 to 5,000 increases the thrust generated from 7.9 kgf to 12.3 kgf and increases the power required from 1.5 kW to 2.9 kW; a result of increasing the angle of attack by reducing the inflow angle (ϕ).

Figure 7 illustrates the effect of changing blade pitch (θ_0) and propeller RPM simultaneously on power and thrust, providing additional insight. Each solid line corresponds to a constant pitch, and the variation along each line (from the solid circle to the solid square) represents an increase in RPM. It was observed that either an increase in RPM or pitch results in an increase in both thrust generated and power consumed (in line with Fig. 6). Additionally, there are multiple combinations of pitch and RPM for a given thrust, albeit at different power levels.

Consider a particular UAV mission where there is a requirement for a thrust increase from 5 kgf to 15 kgf (perhaps transitioning from cruise to hover before landing). This change can be achieved by: 1. increasing the propeller RPM from 3,200 to 5,500 (marked Point A to Point B in Fig. 7) at a constant

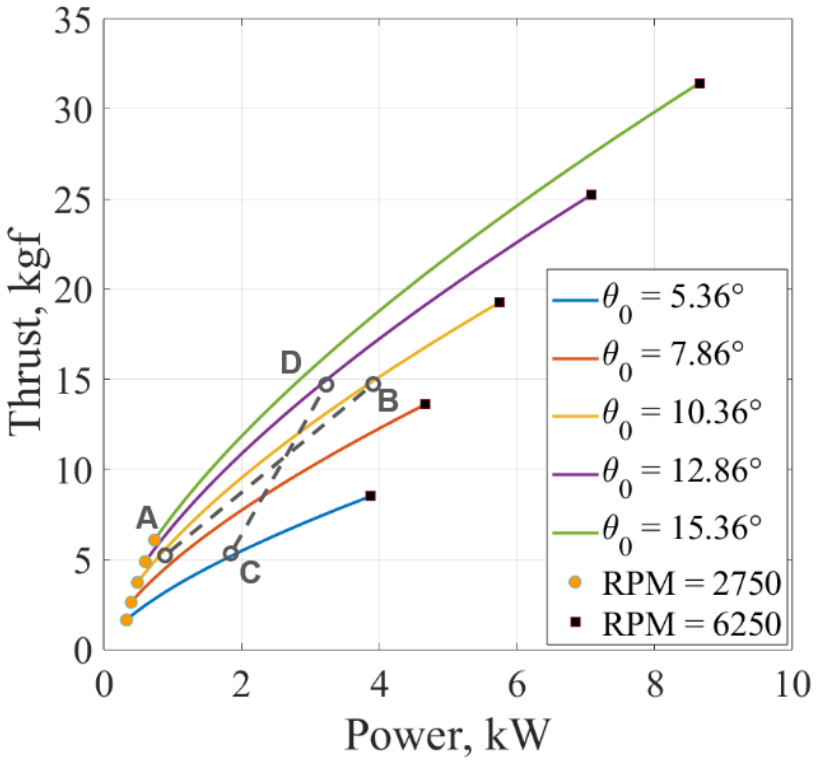

Fig. 7 Variation of thrust vs power required at different pitch angles (referenced to 75% span)

blade pitch with the power required increasing from 0.8 kW to 4 kW, or 2. increasing the blade pitch from 5.4° to 12.9° at a constant RPM (Point C to Point D) with the power required increasing from 1.8 kW to 3.2 kW. It is noteworthy that the increase in power required is higher for a change in RPM as opposed to a change in pitch. This change was 2.3 times higher in the aforementioned example. Additionally, for generating the same thrust, maintaining a lower blade pitch with a higher RPM is preferable. With this observation, it can be understood that introducing blade pitch change even for the case of hover provides better control over thrust generated and power consumed.

3.2 Effect of forward speed:

This section explores the effect of forward flight speed on the thrust and power of the propeller. The Vc or climb velocity is considered for forward speed as the flight conditions considered are axial only. It is noted that any change in forward flight speed will alter the out-of-plane velocity (see Fig. 2) and will subsequently change the inflow angle (ϕ) and the angle of attack (α). Figures 8(a) and 8(b) show the effect of forward speed on the thrust and aerodynamic power required at different RPMs while maintaining a constant blade pitch of 10.4°. As expected an increase in flight speed will decrease the angle of attack for a fixed blade pitch, which in turn will result in a reduction in lift and drag. This reduction is manifested in the loss of thrust and reduction in torque (or power). Qualitatively, the thrust and power trend is similar to that observed in Fig. 7, as the underlying aerodynamics are affected in a similar fashion.

Figure 8(c) shows the effect of Vc simultaneously on thrust and power. For constant power consumption, increasing the Vc decreases the thrust generated. This effect is similar to blade pitch decrease, where the AOA decreases. Here the AOA decreases due to an increase in Vc while the blade pitch remains constant. Increasing Vc from 0 m/s to 12 m/s at a constant power of 4 kW, decreases thrust from 15 kgf to 10 kgf by increasing engine RPM from 5500 to 5700 (from 8(a)). The increase in engine RPM is not sufficient to maintain the thrust for the same power required, hence the thrust generated decreases. Similarly, for generating constant thrust, the power required increases with an increase in Vc. A similar impact of AOA occurs for different climb conditions as well. Similar to the hover condition, at different climb velocities, multiple combinations of θ_0 and RPM are available to produce the required thrust which needs to be determined.

3.3 Optimisation

On an aircraft, the propeller is expected to provide a certain thrust for a given flight condition. Consequently, the blade pitch and RPM are parameters that can be altered to obtain this thrust. However, as seen in Fig. 7, there are multiple combinations of the above to achieve this result. One approach would be to create a factorial search space and interpolate to obtain the values of pitch and RPM. However, in this study, a formal optimisation process is followed where the pitch and RPM are design variables with the goal of minimising power subject to equality and inequality constraints. which can be expressed as

$$f(x_{\text{RPM}}, x_{\theta_0}) = \text{Power required} \rightarrow \min \quad (1)$$

$$g(x_{\text{RPM}}, x_{\theta_0}) = \text{Lift coefficient} - 1.0 \geq 0 \quad (2)$$

$$x_{\text{RPM}} \in [2500, 6500] \quad (3)$$

$$x_{\theta_0} \in [0°, 45°] \quad (4)$$

The advantage of this formulation is the ability to extend the method for over-actuated systems (such as the one studied here) or to deal with failure modes (potential propeller failure). A gradient-based non-linear constrained optimizer [16] was used in the present study. Note that as the current BEMT formulation assumes linear aerodynamics, there is no practical limit on the lift that can be generated. Consequently, inequality constraints are applied to limit the lift coefficient to 1.0 (to account for control

authority in case of gusts, manoeuvres, and other disturbances). Additionally, limits were set on RPM such that it is the range of engine operation.

Figure 9 shows the flowchart of the optimisation process in the present study. Engine power consumed is the parameter that needs to be optimised for its minimum value, as shown in Fig. 9. Previously validated BEMT theory will be used for the calculations. Operating RPM range and pitch range are the assumed mechanical constraints of the system, which will be the boundary conditions for the optimiser. The coefficient of lift is another boundary condition that ensures the blade does not exceed the stall limit

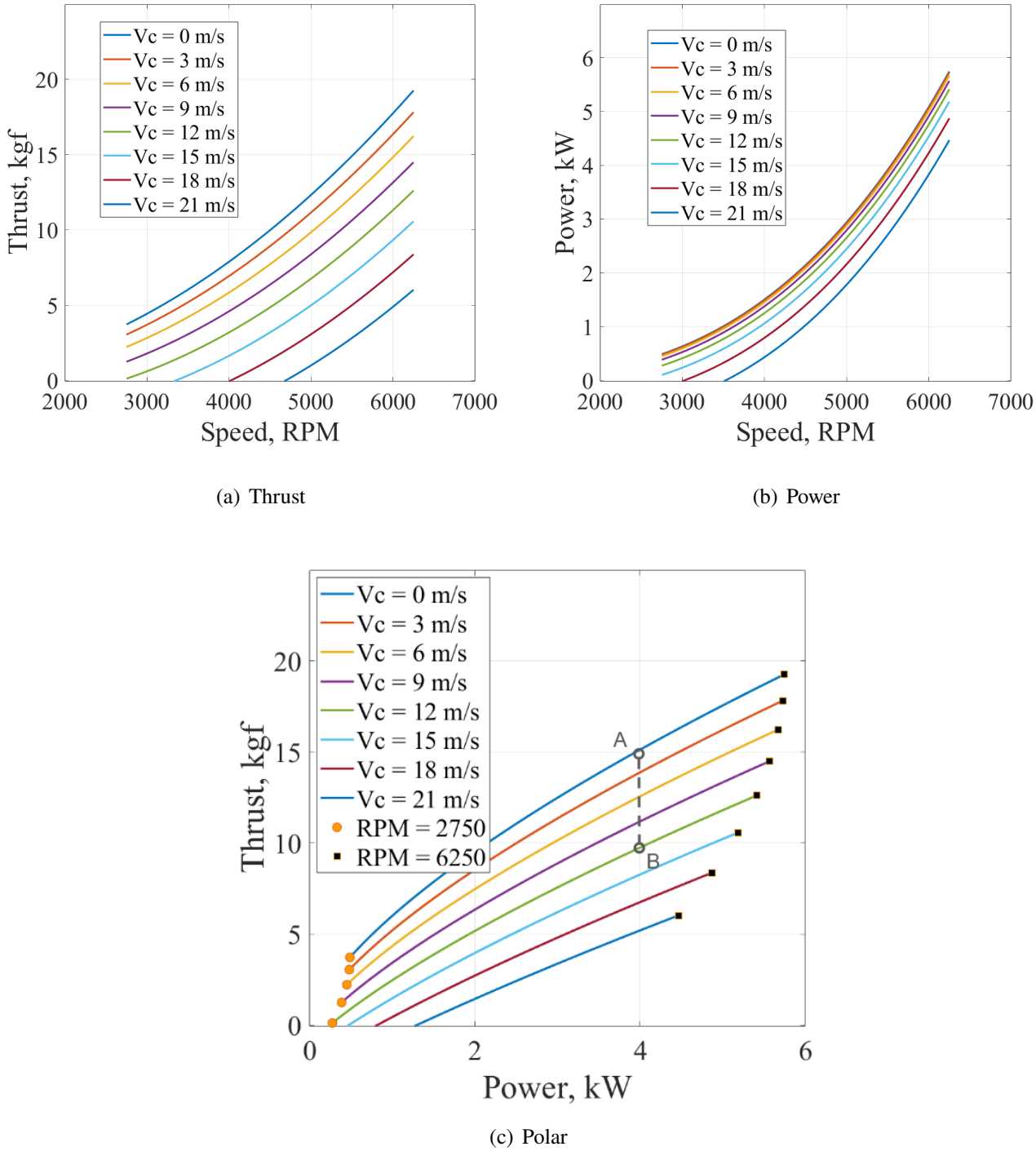

(a) Thrust

(b) Power

(c) Polar

Fig. 8 Variation in thrust and power as a function of RPM and forward flight speed.

during an increase in pitch. Required thrust is also given as an additional constraint. Finally, the optimiser will estimate the values of RPM and pitch of the propeller to be maintained after iterating for minimum power within the limits specified.

The optimised results for different thrust values are shown in Fig. 10, where the optimum RPM and pitch values at different thrust conditions for hover and a climb velocity of 25 m/s. It is evident from Fig. 10 that the θ_0 for the climb condition is higher for all thrust values when compared with the hover, which is required to compensate for the decreased angle of attack due to an increase in the climb velocity.

Assuming a configuration where the same propeller is expected to produce thrust in hover and overcome drag in forward flight, two notional conditions were chosen: 1. Hover at a thrust of 30 kgf, and 2. Forward flight (axial climb) at 25 m/s producing a thrust of 5 kgf (assuming a vehicle L/D of 6). Table 1 compares the hover and the climb condition with the values of thrust, V_c, θ_0, speed and power required. Furthermore, for an axial climb of V_c = 25 m/s, the RPM required is lower than the hover condition because of lesser thrust. For the same case, the θ_0 required is higher because of the necessity to increase the angle of attack to match the required thrust. Similarly, for V_c = 0 m/s, the thrust required is higher, which is 30 kgf; hence, the RPM is higher, but the pitch is lower because of lower V_c. The effect of pitch and RPM on the power required can be observed in Table 1. Finally, for the cases studied here, the highest pitch value observed in the hover case is not in the operating range for the V_c = 25 m/s case. If the pitch of the propeller were not variable, it would not be possible for the propeller to produce the thrust for such a higher V_c.

Table 1 Optimised results for hover and climb condition

Thrust, kgf	Forward speed, V_c, m/s	Blade pitch, θ_0, deg	Propeller RPM	Power required, kW
15	0	9.5	5,750	4.2
5	25	28.0	2,900	1.8

3.4 Powertrain Design

This section illustrates the differences between the two powerplant architectures used in UAVs; an all-electric powertrain where a battery powers the propellers through a motor and speed controller combination, and a direct drive IC engine. The powertrain diagram for both is shown in Fig. 11. The focus is to assess the powerplant weight of both these architectures for a notional UAV mission. Such a tradeoff study can better illustrate the effectiveness of a direct drive IC engine.

Various weight models are considered for the battery, motor, engine and fuel, and the same are shown in Fig. 12 against the power required.

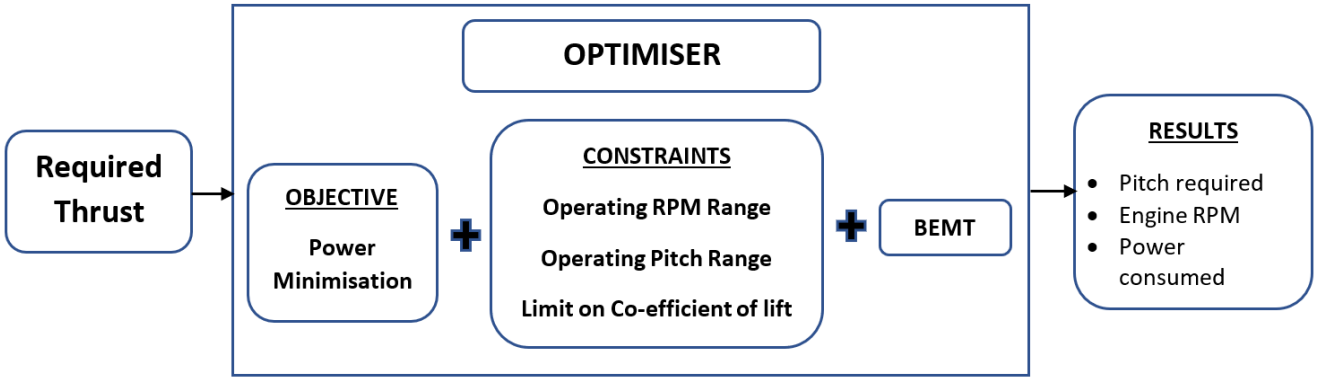

Fig. 9 Flow Chart of steps in Optimisation

Motor and Speed Controllers: The motor and ESC weights are obtained from collecting data from commercial off-the-shelf components, as shown in Fig. 12(b), and a linear fit was obtained between mass and power output. The mass of the motor+speed controller is estimated at 0.25 kg/kW of peak output shaft power. A combined motor+speed controller efficiency of 86% was used to calculate battery output power.

$$M_{\text{motor+ESC}}\ (\text{in kg}) = 0.25\ \text{P}\ (\text{in kW}), \quad \text{P} \leq\ 10\ \text{kW} \tag{5}$$

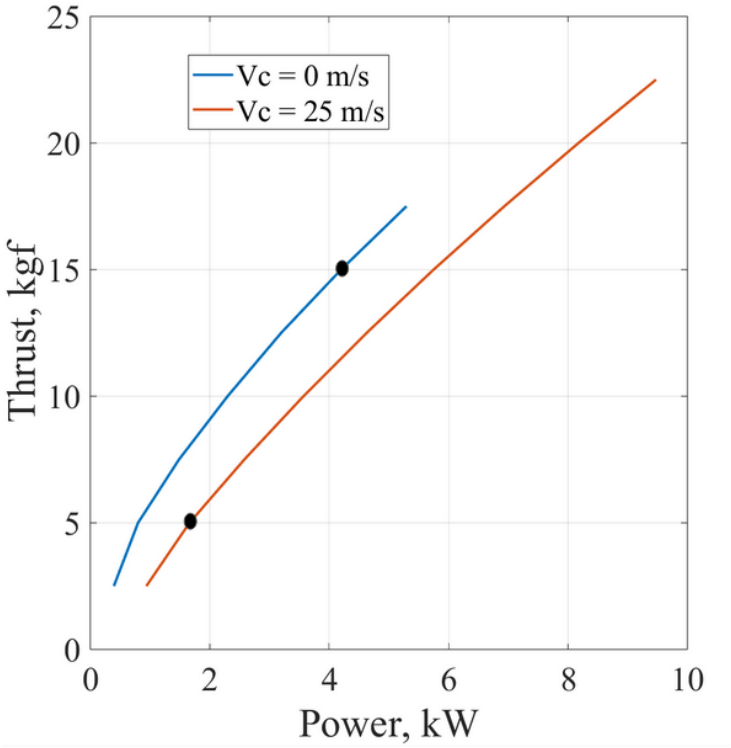

(a) Thrust

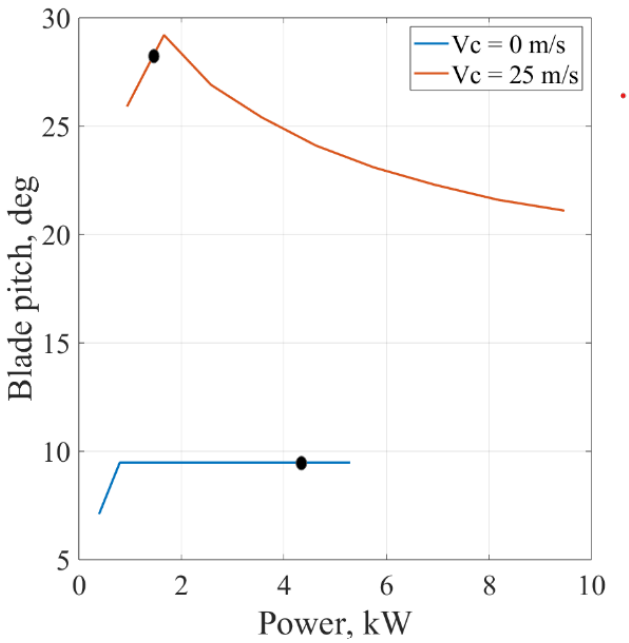

(b) Blade pitch

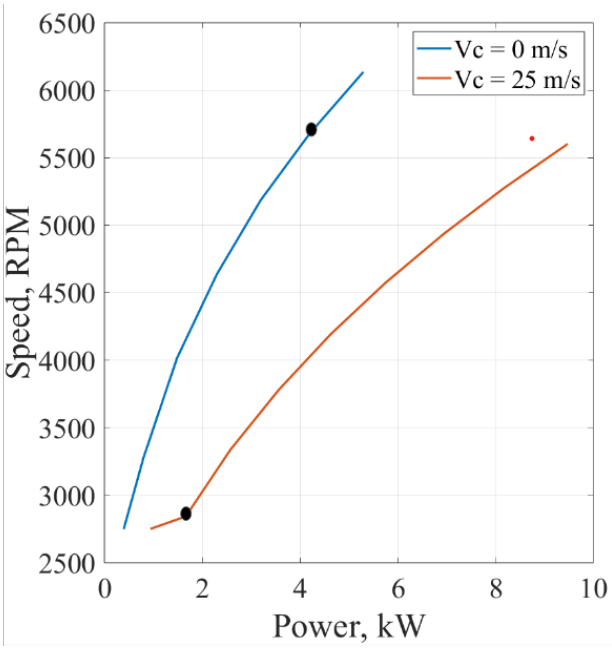

(c) Speed

Fig. 10 Variation in thrust and power as a function of RPM and forward flight speed.

Table 2 Predicted weights of powertrain components

Mission	RPM	Blade pitch θ_0, deg	Power required, kW	Electric		Direct Drive IC	
				W_{battery} kg	$W_{\text{motor+ESC}}$ kg	W_{ICengine} kg	W_{fuel} kg
Hover	5,750	9.5	4.2	3.15	1.3	2.1	0.16
Cruise	2,900	28.0	1.8	4.20	0.43	1.10	0.22
			Total	9.08 kg		3.58 kg	

Battery: The mass of the battery was calculated using the required output pack energy together with assumed values or pack-specific energy (158 Wh/kg). Discharge efficiency losses due to high C-rates, as well as capacity fade due to repeated charge/discharge and cutoff voltage considerations were folded into the pack-level specific energy metric. The values of required output energy are based on assumed motor+speed controller efficiencies (86%).

IC Engine: A database of existing commercial-off-the-shelf (COTS) IC engines were collected, and the variation in mass and specific fuel consumption with engine rating are shown in Figs. 12(c) and 12(d), respectively. Large engines are classified as those whose maximum power limit is around 250 kW, and small engines are those with a limit of 50 kW and are typically used in hobby-grade applications. The mass of the engine is then computed as:

$$M_{\text{ICengine}}\ (\text{in kg}) = \begin{cases} 0.9009\ \text{P} + 6.9540, & \text{Large engines (P} < 250\ \text{kW)} \\ 0.3422\ \text{P} + 0.5254, & \text{Small engines (P} < 50\ \text{kW)} \end{cases} \tag{6}$$

The specific fuel consumption (data available only for the larger engines) is given by,

$$\text{SFC (in kg/kW-hr)} = 6.665 \times 10^{-6} P^2 - 2.219 \times 10^{-3} P + 0.3963 \tag{7}$$

To evaluate the effect of a variable pitch IC engine, the mission considered in Table 1 is revisited. The effect of an IC engine is highlighted by comparing the two powertrain architectures, as shown in Fig. 11, i.e., an all electric and a direct drive IC engine. The weights of the powertrain components are calculated and presented in Table 2.

Considering the all-electric system, the battery weight required in the hover segment is 2.2 kg and that in the cruise segment is 4.2 kg. The motor-ESC combination is sized by the hover segment, which draws a higher power. Consequently, the motor-ESC weighs 1.3 kg with the total powertrain weighing 9.08 kg. In contrast, the IC engine weight is 2.1 kg (again sized by hover), but the overall fuel weight

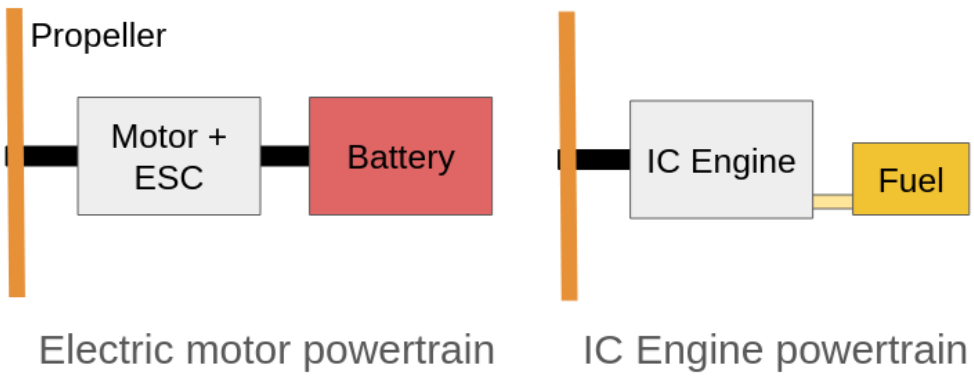

Fig. 11 Two powertrain architectures considered; an electric and direct drive IC engine.

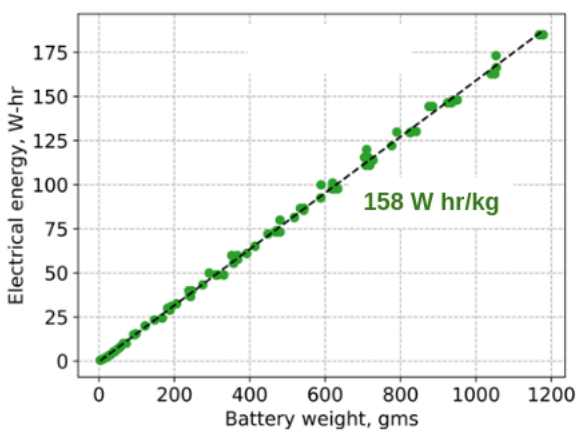

(a) Battery mass

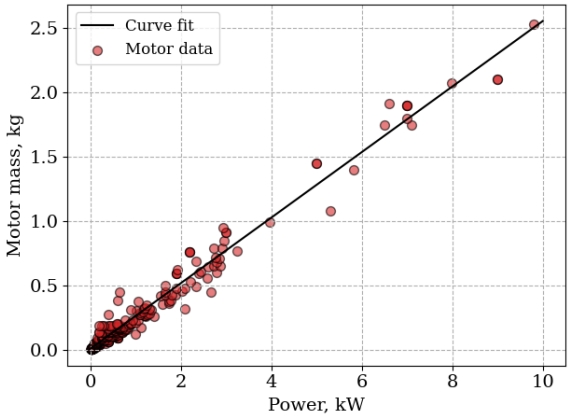

(b) Motor mass

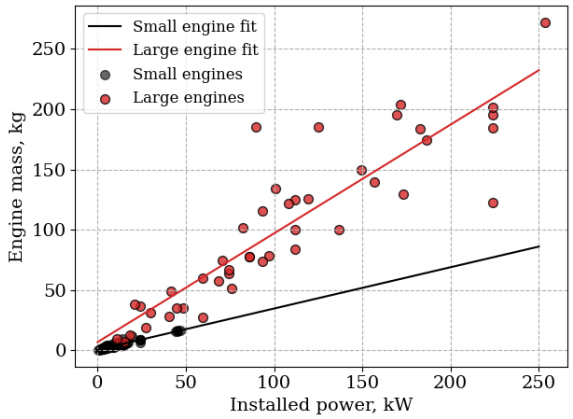

(c) Engine mass

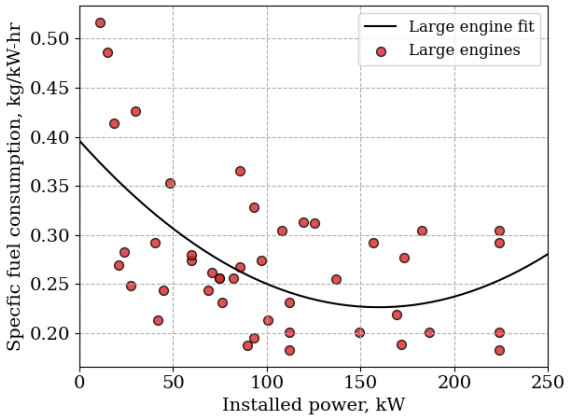

(d) Engine SFC

Fig. 12 Model for powerplant weights

is only 0.38 kg owing to the much higher specific energy of hydrocarbon fuels compared to batteries. Therefore, the direct drive IC engine system weighs 3.58 kg. It should be noted that there are three factors that result in this weight difference: 1. Variable pitch propellers, 2. Variable RPM systems, and 3. The higher specific energy density of hydrocarbon fuels.

4 Conclusion

The study focuses on understanding the effects of pitch and RPM on the aerodynamic performance of the blade. The present study uses a gradient-based optimiser in conjunction with a blade element momentum theory formulation to model propeller aerodynamics. Specific conclusions drawn from this study are

1) There are multiple combinations of blade pitch and RPM to achieve a given thrust, but only one of these corresponds to the lowest power requirement.
2) Changes in blade pitch result in a lower power change compared to changes in RPM, which can significantly change the local dynamic pressure.
3) The optimiser along with the BEMT allows for rapid identification of the optimal pitch-RPM setting for a given thrust and flight condition. The formulation was found to be effective in all the cases considered.

4) The inclusion of a direct drive IC engine can greatly reduce the system weight owing to the much higher specific energy density of hydrocarbon fuels compared to an all-electric powertrain.

References

[1] K. P. Valavanis. Advances in unmanned aerial vehicles: state of the art and the road to autonomy. 2008.

[2] R. Hugh Stone, Peter Anderson, Colin Hutchison, Allen Tsai, Peter Gibbens, and K. C. Wong. Flight testing of the T-wing tail-sitter unmanned air vehicle. *Journal of Aircraft*, 45(2):673–685, 2008. ISSN: 15333868. DOI: 10.2514/1.32750.

[3] Daisuke Kubo and Shinji Suzuki. Tail-sitter vertical takeoff and landing unmanned aerial vehicle: Transitional flight analysis. *Journal of Aircraft*, 45(1):292–297, 2008. ISSN: 15333868. DOI: 10.2514/1.30122.

[4] Daniel Raymer. *Aircraft Design: A Conceptual Approach, Sixth Edition and RDSwin Student SET*. 2019. ISBN: 0930403517. DOI: 10.2514/4.105746.

[5] Kenneth M. Leishman, J. Gordon; Rosen. Challenges in the Aerodynamic Optimization of High-Efficiency Proprotors. *Journal of the American Helicopter Society,*, 2011. DOI: 10.4050/JAHS.56.012004.

[6] Emil Fresk and George Nikolakopoulos. Experimental model derivation and control of a variable pitch propeller equipped quadrotor. *2014 IEEE Conference on Control Applications, CCA. Part of 2014 IEEE Multi-conference on Systems and Control, MSC 2014*, pages 723–729, 2014. DOI: 10.1109/CCA.2014.6981426.

[7] Brandyn Phillips, Vikram Hrishikeshavan, Omri Rand, and Inderjit Chopra. Design and development of a scaled quadrotor biplane with variable pitch proprotors for rapid payload delivery. *Annual Forum Proceedings - AHS International*, 1(August):302–315, 2016. ISSN: 15522938.

[8] Maciej Podsędkowski, Rafał Konopiński, Damian Obidowski, and Katarzyna Koter. Variable pitch propeller for UAV-experimental tests. *Energies*, 13(20):1–16, 2020. ISSN: 19961073. DOI: 10.3390/en13205264.

[9] Jianhua Xu, Wenping Song, Xudong Yang, and Han Nie. Aerodynamic Performance of Variable-Pitch Propellers for High-Altitude UAVs. *IOP Conference Series: Materials Science and Engineering*, 686(1), 2019. ISSN: 1757899X. DOI: 10.1088/1757-899X/686/1/012019.

[10] Variable-pitch Gasoline-engine Quadrotor, Tao Pang, Kemao Peng, Feng Lin, and Ben M Chen. Towards Long-endurance Flight : Design and Implementation of a. 2016.

[11] Travis Henderson and Nikolaos Papanikolopoulos. Power-minimizing control of a variable-pitch propulsion system for versatile unmanned aerial vehicles. *Proceedings - IEEE International Conference on Robotics and Automation*, 2019-May:4148–4153, 2019. ISSN: 10504729. DOI: 10.1109/ICRA.2019.8794357.

[12] Vishnu S. Chipade, Abhishek, Mangal Kothari, and Rushikesh R. Chaudhari. Systematic design methodology for development and flight testing of a variable pitch quadrotor biplane VTOL UAV for payload delivery. *Mechatronics*, 55:94–114, 2018. ISSN: 09574158. DOI: 10.1016/j.mechatronics.2018.08.008.

[13] J Gordon Leishman. *Principles of helicopter aerodynamics*. 2006.

[14] S. Raviteja. UMS Radial Engine Report. Technical report, 2017.

[15] Shrivathsan Narayanan, Aaditya Chandel, and Bharath Govindarajan. Effect of Gust on Coaxial Rotors using Free Vortex Methods. 80th Annual Forum of the Vertical Flight Society Montréal, Québec, Canada, 2024.

[16] Richard H. Byrd, Mary E. Hribar, and Jorge Nocedal. An interior point algorithm for large-scale nonlinear programming. *SIAM Journal on Optimization*, 9(4):877–900, 1999. ISSN: 10526234. DOI: 10.1137/S1052623497325107.